AECL-6965

ATOMIC ENERGY OF CANADA LIMITED

L'ÉNERGIE ATOMIQUE DU CANADA LIMITÉE

EDDY CURRENT DETECTION OF CORROSION DAMAGE IN HEAT EXCHANGER TUBES

Détection par courants de Foucault des dommages dus à la corrosion dans les tubes des échangeurs de chaleur

G. VAN DRUNEN, V.S. CECCO and J.R. CARTER

Chalk River Nuclear Laboratories *Laboratoires nucléaires de Chalk River*

Chalk River, *Ontario*

May 1980 mai

ATOMIC ENERGY OF CANADA LIMITED

EDDY CURRENT DETECTION OF CORROSION DAMAGE IN HEAT EXCHANGER TUBES

by

G. Van Drunen, V.S. Cecco and J.R. Carter

Chalk River Nuclear Laboratories
Chalk River, Ontario
1980 MAY

AECL-6965

L'ÉNERGIE ATOMIQUE DU CANADA, LIMITÉE

Détection par courants de Foucault des dommages dus à la corrosion dans les tubes des échangeurs de chaleur

par

G. Van Drunen, V.S. Cecco et J.R. Carter

RÉSUMÉ

Les courants de Foucault constituent souvent la meilleure méthode d'essais non destructeurs que l'on peut employer pour l'inspection en cours de service des tubes à faible alésage des échangeurs de chaleur. On décrit dans les grandes lignes, les principes de base ainsi que les avantages et les inconvénients de cette méthode. On présente des indications typiques données par les courants de Foucault en ce qui concerne les défauts découlant de la corrosion comme la fissuration par corrosion sous tension, le piquage et la bosselure des tubes sous les plaques de support. Les signaux des courants de Foucault provenant de caractéristiques comme les dépôts de magnétite et les inclusions ferromagnétiques pouvant être erronément pris pour des défauts font également l'objet de commentaires.

Ce rapport a été présenté à la réunion de la région Est de NACE (National Association of Corrosion Engineers) ayant eu lieu du 2 au 4 octobre 1979 en l'hôtel Skyline à Ottawa, Ontario.

Laboratoires nucléaires de Chalk River
Chalk River, Ontario

Mai 1980

AECL-6965

ATOMIC ENERGY OF CANADA LIMITED

EDDY CURRENT DETECTION OF CORROSION DAMAGE IN HEAT EXCHANGER TUBES

by

G. Van Drunen, V.S. Cecco and J.R. Carter

ABSTRACT

Eddy current is often the most effective nondestructive test method available for in-service inspection of small bore tubing in heat exchangers. The basic principles, advantages and shortcomings of the technique are outlined. Typical eddy current indications from corrosion-related defects such as stress corrosion cracks, pitting and tube denting under support plates are presented. Eddy current signals from features such as magnetite deposits and ferromagnetic inclusions which might be mistaken for defects are also discussed.

This paper was presented at the National Association of Corrosion Engineers (NACE) Eastern Region Conference, October 2-4, 1979, Skyline Hotel, Ottawa, Ontario

Chalk River Nuclear Laboratories
Chalk River, Ontario
1980 MAY

AECL-6965

CONTENTS

TABLES

FIGURES

1. INTRODUCTION

The need for high energy efficiency in heat exchangers does not readily permit an increase in material thickness for corrosion allowance. This requirement, coupled with the very large surface areas involved (up to 2500 m^2 in a 150 MW nuclear boiler) makes corrosion an important consideration in heat exchanger design and operation.

Corrosion is important to the CANDU reactor system because a reactor may contain 20 or more heat exchangers whose failure requires station shutdown. Many of these heat exchangers are exposed to once-through lake or river water. In addition, AECL is concerned with heavy water production which involves exposure of heat exchangers to the extremely corrosive conditions of combined heat, moisture and hydrogen sulphide.

This report deals with nondestructive detection of various types of corrosion-related defects in thin walled tubes by eddy current testing (ECT). No attempt is made to examine details of corrosion processes - this area is left to experts in the corrosion field. Over the past decade ECT has evolved as a valuable NDT technique. Present practice involves manual or mechanized scanning of a single tube combined with visual analysis of test results. This approach will be illustrated. However, it should be mentioned that ongoing research and development in the areas of automated tube scanning, automated signal analysis and multifrequency test techniques are expected to improve the effectiveness and increase applications for ECT, particularly for large test programs.

The first part of the report outlines the physical basis for the eddy current technique. Subsequently, a number of real corrosion examples are presented which illustrate the capabilities and limitations of the method. Only some examples are from nuclear installations, the rest came from thermal power stations and other types of industrial heat exchangers. A few cases will also be presented of anomalous signals demonstrating the need for a thorough understanding of ECT if reliable results are to be obtained.

2. EDDY CURRENT TESTING

2.1 Background

Eddy current testing normally involves measurement of impedance or changes in impedance of a test coil. When

alternating current is passed through a coil (Figure 1) an alternating primary magnetic field, H_o, results. Eddy currents are induced in a conductor in proximity to the coil due to the varying nature of H_o, these eddy currents in turn have an associated magnetic field, H_i. In non-ferromagnetic materials H_i opposes and partially cancels H_o. Impedance (both reactive and resistive components) of the coil changes with H_i and the magnitude of H_i depends on the eddy current density, J. Any parameter which affects J will be reflected as a coil impedance change. Such parameters are:

i) coil to specimen spacing (lift-off)
ii) resistivity of the material
iii) geometrical factors (defects, shape).

A fourth factor which influences coil impedance is magnetic permeability. The presence of ferromagnetic material increases the magnetic flux lines which link the test coil increasing its inductance whereas non-magnetic materials always result in decreasing inductance. Testing of ferromagnetic materials is outside the scope of this report. There are two important fundamental properties of eddy currents which have to be considered during ECT, skin effect and phase lag.

Skin effect describes the reduction in eddy current density below the test material surface. In an infinitely thick material current density (J) decreases exponentially as shown in Figure 2(a). The depth where J has dropped to 1/e or 37% of the value at the surface is defined as the standard depth of penetration or skin depth, δ, given by

$$\delta = (\rho/\pi f \mu)^{\frac{1}{2}}$$

or

$$\delta \tilde{=} 50\ (\rho/f\mu_r)^{\frac{1}{2}}$$

where ρ is resistivity in microhm-centimetres, f is test frequency in hertz and μ_r is relative magnetic permeability. Decreasing eddy current density with depth could be a severe handicap to ECT since small surface defects and large sub-surface defects would have a similar effect on test coil impedance. Fortunately, phase lag offers a solution.

Phase lag, β, is the time delay (under equilibrium conditions) between sinusoidal eddy currents at the surface and those at depth x below the surface. In an infinitely thick material β varies linearly with depth (Figure 2(b)) and is given by

$$\beta = x/\delta \text{ radians}$$

One can distinguish deep from shallow defects because of phase lag.

2.2 Test Equipment

Since defects normally yield only small changes in coil impedance the test coil is usually made part of a bridge circuit as shown in Figure 3. Two types of test probes are in common use. An absolute probe, Figure 3(b), has the balancing or reference coil (Coil 2) remote from the test material, either in the probe body as shown or in the instrument. A differential probe has two identical coils which couple equally to the test material at different locations, Figure 3(c). Both types of probes are initially balanced in contact with sound test material. As the sensing coil in an absolute probe passes a defect the resulting out-of-balance condition will cause a deflection of the voltmeter. When differential coils pass a defect the voltmeter will deflect in one direction as the first coil senses the defect, the meter will read zero (bridge balanced) when both coils sense the defect equally and the meter will deflect in the opposite direction when only the second coil is over the defect.

There are advantages and disadvantages to both absolute and differential probes. These are summarized in Table I. Experience at CRNL has shown that the advantages of absolute probes outweigh the disadvantages, absolute probes are therefore used for the majority of tests, and differential probes only in certain circumstances. The examples to follow will illustrate some of the more serious shortcomings of differential probes.

Simple EC instruments usually operate at fixed frequency (resonance) and have an analog meter output. Such instruments have several disadvantages. Fixed or limited choice of operating frequency means penetration depth is not controllable. An analog output may not differentiate between real defects and harmless variations in properties

such as resistivity and magnetic permeability. Modern EC instruments utilize both the amplitude and phase of the eddy currents. This is accomplished by replacing the voltmeter in Figure 3(a) with phase discrimination circuits and presenting the results on a cathode ray tube (CRT). There is a close relationship between phasor diagrams of sinusoids and impedance diagrams so the display can be visualized as showing the reactive component of the sensing coil impedance along the vertical axis and the resistive component along the horizontal axis. By this means both amplitude and phase of the out-of-balance eddy current signal from a defect can be monitored. Such instruments also permit test frequency to be varied, typically over a range from 100 or 1000 Hz to over 2 MHz.

The effect of changes in test and material properties on an eddy current impedance display is illustrated in Figure 4. It shows the impedance loci at 5 kHz of a coil, initially balanced in air, as it is brought into contact with materials of decreasing resistivity (increasing conductivity). The inset figure shows the effect of variation in thickness. Note the angular separation between the lift-off, resistivity and thickness directions. Features 1 and 2 in the inset figure are both the result of a decrease in thickness, the angular separation between 1 and 2 is due to phase lag.

Figure 4 suggests several applications of ECT as a nondestructive test method. The sensitivity to lift-off can be used to measure the thickness of nonconducting layers on a conducting substrate, paint or oxide layer thickness, for example. The response to thickness variations provides sensitivity to defects. The variation in coil impedance with changes in resistivity permits comparison testing for material sorting applications.

The results of Figure 4 were obtained with a surface (pancake) probe but comparable results are obtained with tube samples and an internal probe such as in Figure 3(b). Figure 5 compares the impedance of surface and internal probes as they are placed close to different materials.

The inspection of thin-walled tubing is the major application of ECT to the detection of corrosion damage in heat exchangers. In-service tube inspection is nearly always accomplished from the inside of the tube with circumferentially wound internal probes such as those in Figure 3.

Probes are attached to the end of a flexible, hollow plastic or metal push cable containing the coil wire connections to the instrument. The probe cable can be pushed through tubes manually or, when large numbers of tubes have to be tested, with a mechanical probe drive.

Eddy current inspection is a comparative test; signals from real defects are compared to artificial calibration defect signals to establish type and depth. The calibration and inspection results are normally recorded on twin channel chart and often in more condensed form on magnetic tape.

The response of an absolute eddy current probe to typical calibration defects is shown in Figure 6. The impedance display has been rotated relative to Figure 4 to make the signal from a defect on the outside of the tube (O.D. defect) vertical, and an I.D. defect nearly horizontal; a through-wall defect will fall about halfway between. The test frequency chosen to obtain this defect presentation is f_{90} , the frequency that will yield about 90^{o} phase separation between I.D. and O.D. defect signals. For thin-wall tubes, f_{90} is given approximately when

$$t = 1.1\delta$$

or

$$f_{90} = \frac{3000\rho}{t^2} \quad \text{Hz}$$

where δ is skin depth, ρ is resistivity in microhm-centimetres and t is wall thickness in mm. At f_{90} all defect signals contain a -Y component. This is more apparent on the X and Y channel chart recordings against time (time =distance at constant probe speed) in Figure 6. All defects yield signals in the fourth quadrant; features such as tube support plates, dents, etc. can be distinguished by their angular relationship to the lift-off (fill-factor) direction.

One can arrive at a qualitative understanding of the characteristic defect signals in Figure 6 if one starts with a +X shift in balance point for increased lift-off and a -Y deflection for an O.D. defect at f_{90}. A dent

places the tube material in closer proximity to the test coil resulting in improved coupling or a shift of the balance point in the -X direction. An I.D. defect represents loss in wall thickness combined with reduced coupling yielding both -Y (loss of wall) and +X (increasing lift-off) deflection. By similar reasoning a through-wall hole should fall between the extremes of I.D. and O.D. defects since it possesses components of both. A tube support plate appears as tube wall thickening, +Y, modified by the difference in resistivity between the tube and support plate materials, the increasing phase lag of the eddy currents in the plate, and in the case of steel supports, the magnetic permeability of the plate material.

3. EXAMPLES OF CORROSION DEFECTS

Initially four examples of corrosion on inside and outside tube surfaces are presented. These are quite easy to compare to calibration signals because the defects are isolated, their signals are not modified or distorted by corrosion products and/or tube support plates. Subsequently, examples are shown of defects at tube supports. These are more complicated because extraneous signals are superimposed on those from defects. Although the accompanying figures only illustrate the tubes, where applicable, eddy current results are obtained with a baffle plate in position to duplicate as closely as possible the inspection results one would obtain during in-service testing.

3.1 External Corrosion

Figure 7 shows corrosion on the outside of a copper tube. The attack is general but non-uniform with localized severe pitting (arrows). An absolute internal probe was used. Eddy current signals from artificial defects and three of the localized pits are shown in Figures 7(b) and (c). The amplitude of the first two corrosion indications is about twice that from a 0.25 mm calibration defect indicating a depth of 0.5 mm, in excellent agreement with the mechanical measurements listed under the defect signals. Note the phase angle shift between the 0.5 mm deep pits and the 0.75 mm pit. The angle of the latter approaches that of a through-wall hole, both the amplitude and phase angle of this defect indicate its severity.

3.2 Internal Corrosion Pitting

Figure 8 shows isolated internal corrosion pits in a Type 316 stainless steel tube removed from a heavy water plant heat exchanger. After testing with an absolute probe the tube was sectioned to enable the photograph in Figure 8(a) and mechanical depth determination. Eddy current signals from calibration defects and corrosion pits are illustrated in Figures 8(b) and (c). Comparison of defect signals with calibration defects reveals that a 0.4 mm deep pit yields a similar signal to the 0.1 mm machined groove. This could result in underestimation of defect depth and points out the need for limited destructive examination to define defect geometry if accurate depth estimates are desired. Note that 0.4 mm deep pitting in Figure 8 is still less than 25% wall loss. More than 25% loss will be apparent from the defect signal phase angle; compare the 0.4 mm and 0.5 mm pit signals.

An example of more general but less deep internal pitting is shown in Figure 9. The material is brass. Calibration signals and the eddy current signals from a few representative defect areas are shown in Figures 9(b) and (c), respectively.

3.3 Stress Corrosion Cracking

An example of stress corrosion cracking (SCC) in Type 316 stainless steel, from a heavy water plant heat exchanger, is shown in Figure 10. The crack extends nearly halfway around the tube. Calibration defect and crack signals are shown in Figures 10(b) and (c). Note that instrument gain had to be reduced from previous examples to display the entire crack signal. The phase angle of the crack indication shows it extends through the tube wall.

The large crack signal is due entirely to the component of the crack along the tube axis. Eddy currents in the tube flow parallel to current in the probe coil. Since a defect must disrupt eddy current flow to be detectable, it follows that a perfectly circumferential crack cannot be detected with a circumferential probe design. The intergranular, branching nature of SCC generally permits their detection. If cracks oriented perpendicular to the tube axis are suspected, fatigue cracks for example, special probes have been designed at CRNL to overcome this difficulty.

3.4 Erosion/Corrosion at Tube Supports

Figure 11 shows an example of erosion/corrosion on either side of a baffle plate in a brass tube from a thermal power station heat exchanger. Damage consists of smooth grooves on either side of the support with complete wall penetration at one point (arrow). Calibration signals are presented in Figure 11(b) and the indications from the defective area are shown in Figure 11(c). The arrows indicate the eddy current instrument response as the probe traversed from left to right. The complete defect signal consists of two downward loops, A and B, with an upward deflection in between. The upward component is due to the ferromagnetic baffle plate, it differs from the baffle plate calibration signal because of distortion from the defects. Loop A is from the groove containing the hole. The presence of the hole explains the phase angle difference between A and B.

Figure 12 is also a brass heat exchanger tube. This tube appears to have suffered general corrosion as well as erosion/corrosion on either side of the baffle plate. The gradual downward trend of the Y-DISTANCE recording in Figure 12(d) shows that the pronounced grooves at A and B are superimposed on an area of general wall thinning in the vicinity of the support plate. The phase angle of the B signal in Figure 12(c) indicates it extends deeper than groove A even though B has the smaller amplitude. Before leaving this tube note the response of a differential probe to the same defects in Figure 13. The differential probe also senses the presence of the localized grooves, however, the Y-DISTANCE recordings gives no indication of the gradual wall thinning which was apparent in Figure 12. This situation arises because the gradual wall loss occurred over a large distance compared to the spacing between the two sensing coils in the probe and illustrates one of the major disadvantages of differential probes.

3.5 Pitting under a Baffle Plate

A final example of corrosion at a baffle plate is shown in Figure 14. The material is Type 304 stainless steel from a nuclear heat exchanger. Figure 14(a) shows a section of tube with part of the carbon steel support plate still in place; the support shows considerable corrosion. Originally there was about 0.25 mm clearance between the tube and the hole in the plate. Corrosion products have

completely filled the gap leading to the crevice corrosion shown in Figure 14(b) which is a similar tube with the baffle plate removed. Calibration signals are presented in Figure 14(c). The eddy current signal from the baffle plate region of Figure 14(a) is illustrated in Figure 14(d). This apparently simple signal is actually quite complex. The downward component is due to external pitting similar to that in Figure 14(b). The presence of a support plate should result in a +X, +Y signal component; in fact a -X deflection is observed. This is the result of denting of the tube. Denting is circumferential constriction of tubes due to compressive stresses exerted by baffle plate corrosion products (magnetite). The presence of magnetite can also contribute to signal distortion, particularly at low test frequencies. The existence of denting is apparent in the defect signal from the corrosion pits with baffle plate removed as in Figure 14(b).

Denting is of concern because, in addition to complicating eddy current signal analysis, it can lead to further tube damage such as stress corrosion cracking and thermal fatigue since the tubes are no longer free to expand and contract during thermal excursions.

4. ANOMALOUS INDICATIONS

Three examples are presented of eddy current indications which could have been mistaken for defects. They illustrate the need for thorough analysis before concluding that every eddy current signal is a defect.

4.1 Copper Deposits

The first example may be a corrosion-related problem, copper base alloy tubing (believed to be aluminum-bronze) from an air conditioner heat exchanger was found with localized areas of copper plating. Copper was presumably taken into solution in some part of the cooling circuit and redeposited near tube support plates. The deposits are thickest on either side of the support as shown in Figure 15, maximum thickness is 0.05 mm. This tube was tested with both absolute and differential probes. The absolute probe signal has no -Y component indicating no wall loss (no defect). The differential probe signal is not nearly as clear and illustrates another disadvantage of differential probes. Comparison of the deposit signal with calibration signals could easily lead one to conclude the presence of an O.D. defect, particularly if the eddy current results were compressed on X and Y channel recordings as is often the case during in-service inspection.

4.2 Ferromagnetic Inclusion

A second type of anomalous indication results from ferromagnetic inclusions which are occasionally encountered during ECT of non-ferromagnetic materials. These arise from chips or filings from steel tooling and handling equipment that are embedded during manufacture. (The surface of non-magnetic stainless steels and nickel-base alloys can also become magnetic as a result of alloy depletion during oxidation or corrosion). Though one might consider a magnetic inclusion a defect there are several reasons why it is important to identify the origin of an indication. Even very small, perhaps insignificant, magnetic inclusions can yield sizeable eddy current signals because of the extreme sensitivity to magnetic permeability. A second reason to determine defect origin is so measures can be taken to minimize further damage: magnetic inclusions are nearly always manufacturing defects. Fortunately, a relatively simple test procedure permits distinguishing between defects and magnetic inclusions as illustrated in Figure 16. Note that these results were obtained with an external encircling probe; this explains the reversal in appearance of I.D. and O.D. defects from previous examples. A magnetic inclusion will yield a signal whose angular separation from the lift-off direction increases as test frequency is reduced. The response of real defects is just the opposite.

4.3 Magnetite Deposits

Corrosion-related anomalous eddy current indications can result from ferromagnetic corrosion products such as magnetite. Figure 17 shows EC response to magnetic deposits inside an Inconel 600 tube at various test frequencies. As in the previous example the existence of magnetite is verified by lowering test frequency, magnetite signals rotate clockwise whereas defect signals rotate counter-clockwise. Note that one could easily mistake the magnetite signals for real defects at 225 kHz and 50 kHz. The same technique of reducing test frequency can be used to verify the presence of magnetite on the outside of a tube. This approach has been used to measure the height of sludge deposits (containing magnetite) above tubesheets during in-service inspection of vertical heat exchangers.

5. SUMMARY AND CONCLUSIONS

1. Eddy current testing reliably detects the presence of cracks and wall loss due to corrosion in thin-walled tubes.

2. Visual signal analysis allows discrimination between I.D., through-wall and O.D. defects as well as estimation of defect depth of ±15% of wall thickness.

3. Absolute eddy current probes yield signals which are usually easier to interpret than those obtained with differential probes.

4. Gradual defects may not be detected at all with differential probes.

5. Absolute probes permit clear separation between signals from wall loss and copper deposits.

6. Ferromagnetic inclusions and deposits can be differentiated from real defects by re-testing at reduced frequency.

TABLE I

COMPARISON OF ABSOLUTE AND DIFFERENTIAL PROBES

A B S O L U T E P R O B E S

ADVANTAGES	DISADVANTAGES
- respond to both sudden and gradual changes in properties and dimensions	- prone to drift from temperature changes
- combined signals are usually easy to separate (simple interpretation)	- more sensitive to probe-wobble than a differential probe
- show total length of defects	

D I F F E R E N T I A L P R O B E S

ADVANTAGES	DISADVANTAGES
- not sensitive to gradual changes in properties or dimensions	- not sensitive to gradual changes (may miss long gradual defects entirely)
- immune to drift from temperature changes	- will only detect ends of long defects
- less sensitive to probe-wobble than an absolute probe	- may yield signals difficult to interpret

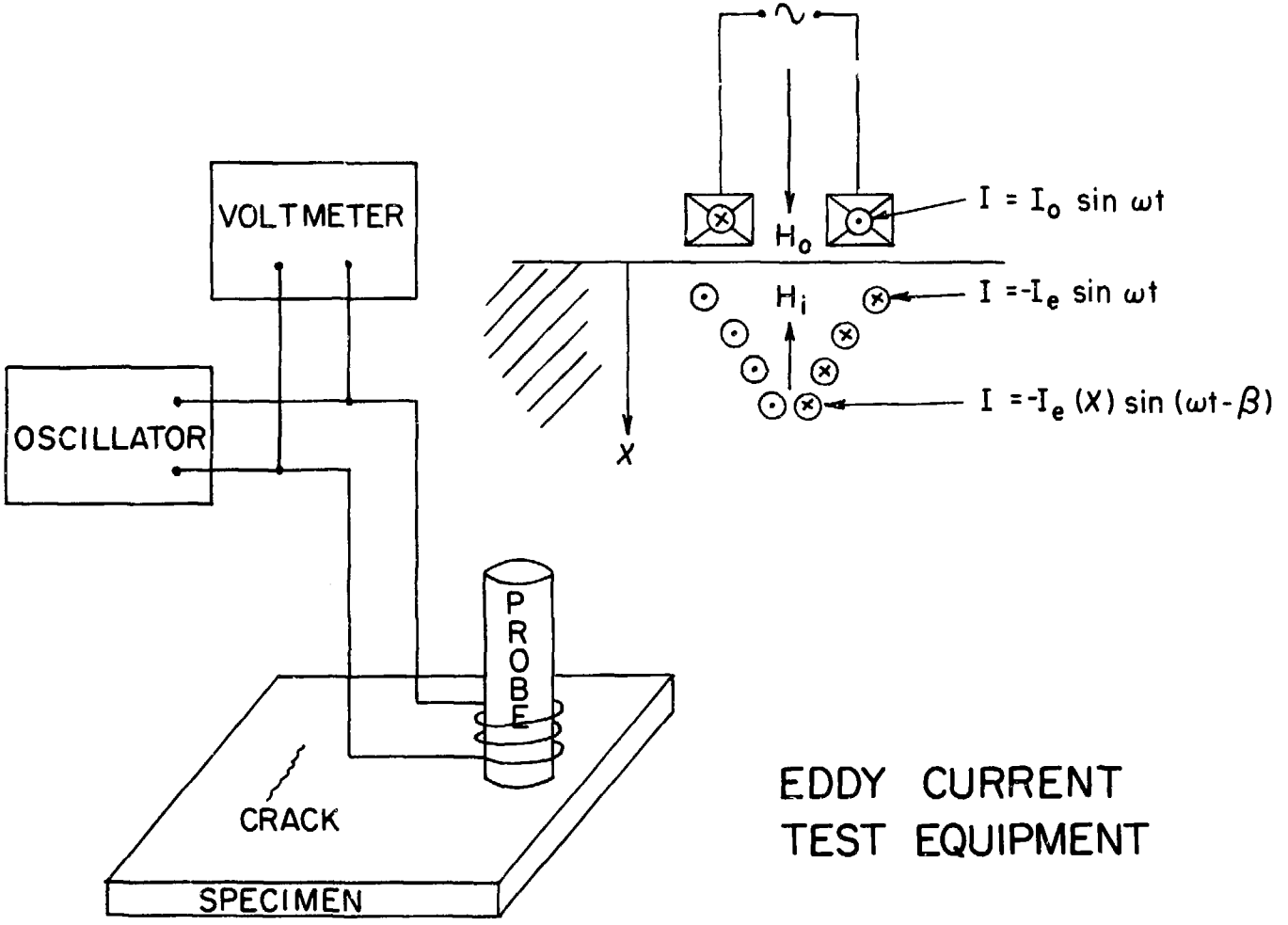

FIGURE 1 Schematic of Simple Eddy Current Instrument

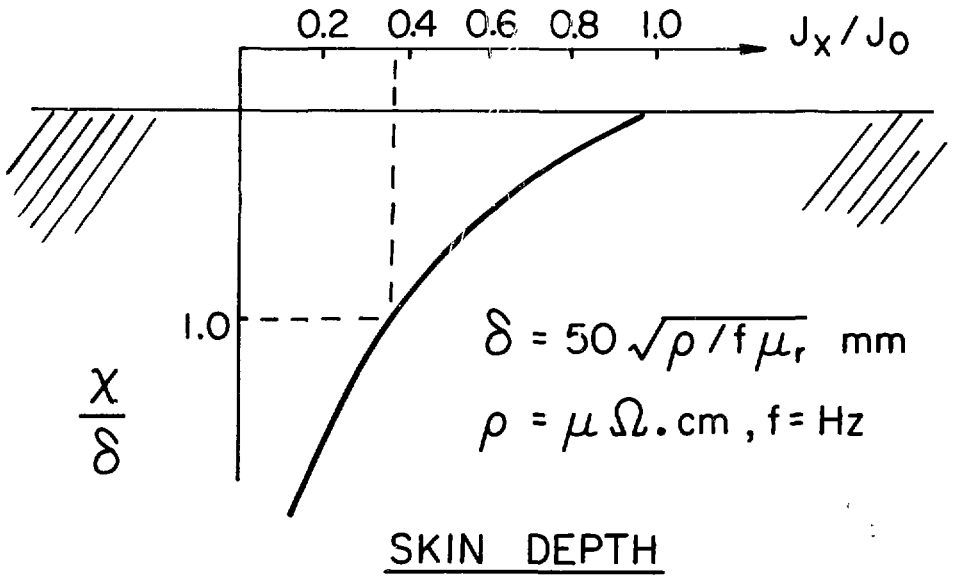

(a)

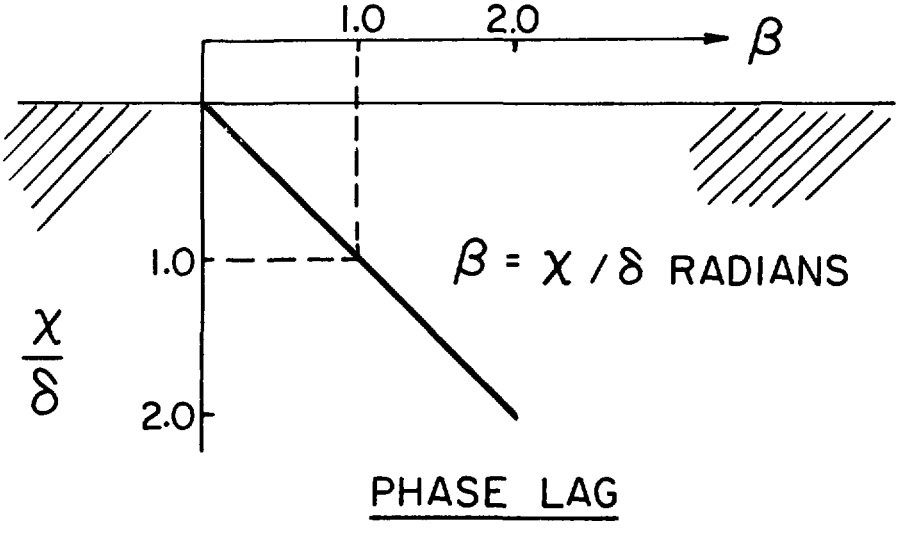

(b)

EDDY CURRENT PARAMETERS

FIGURE 2 Skin Depth and Phase Lag in Infinitely Thick Materials

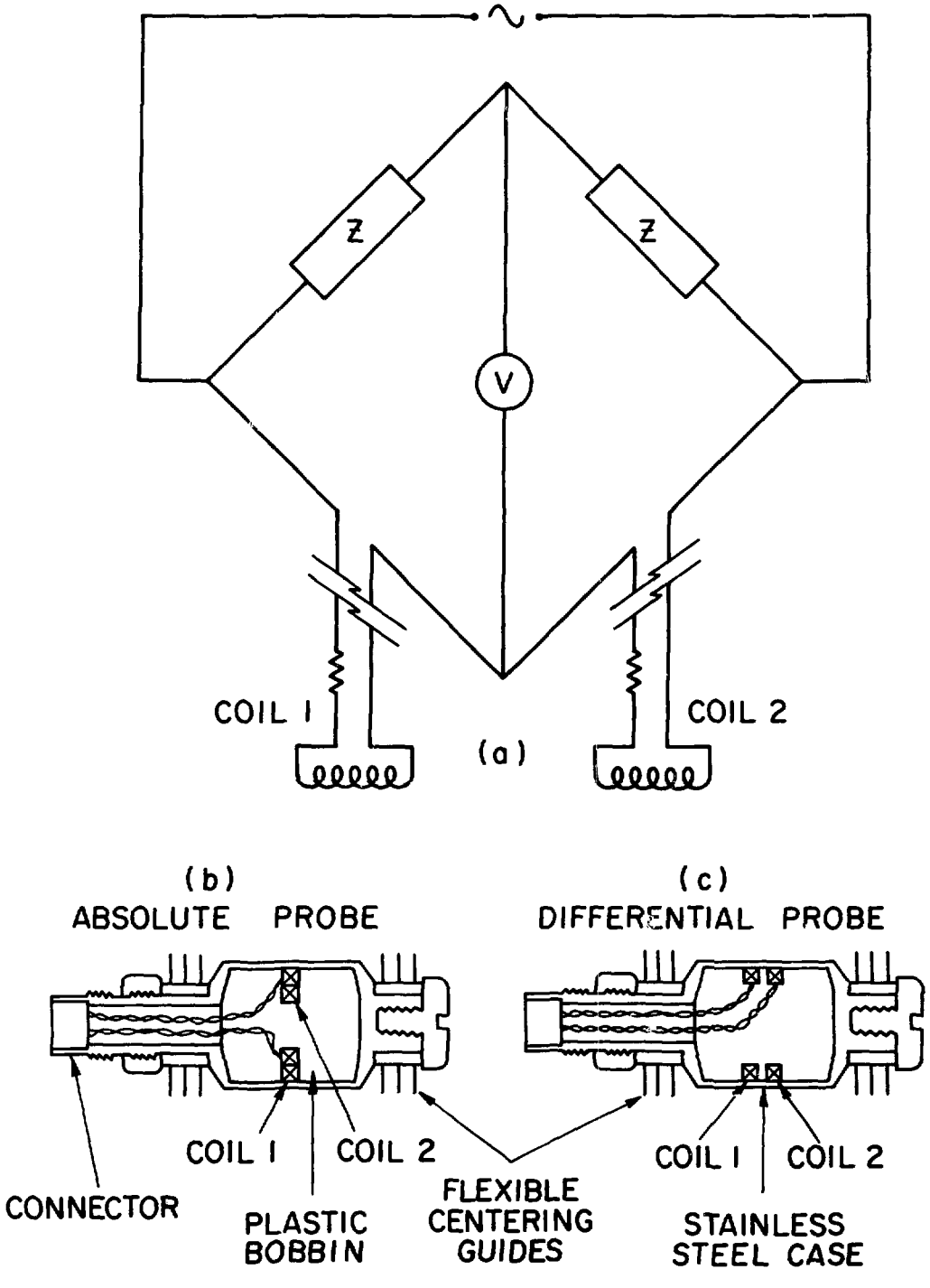

FIGURE 3 (a) Location of probe coils in an A.C. bridge circuit. (b) Absolute and (c) Differential probes for testing tubes from the inside.

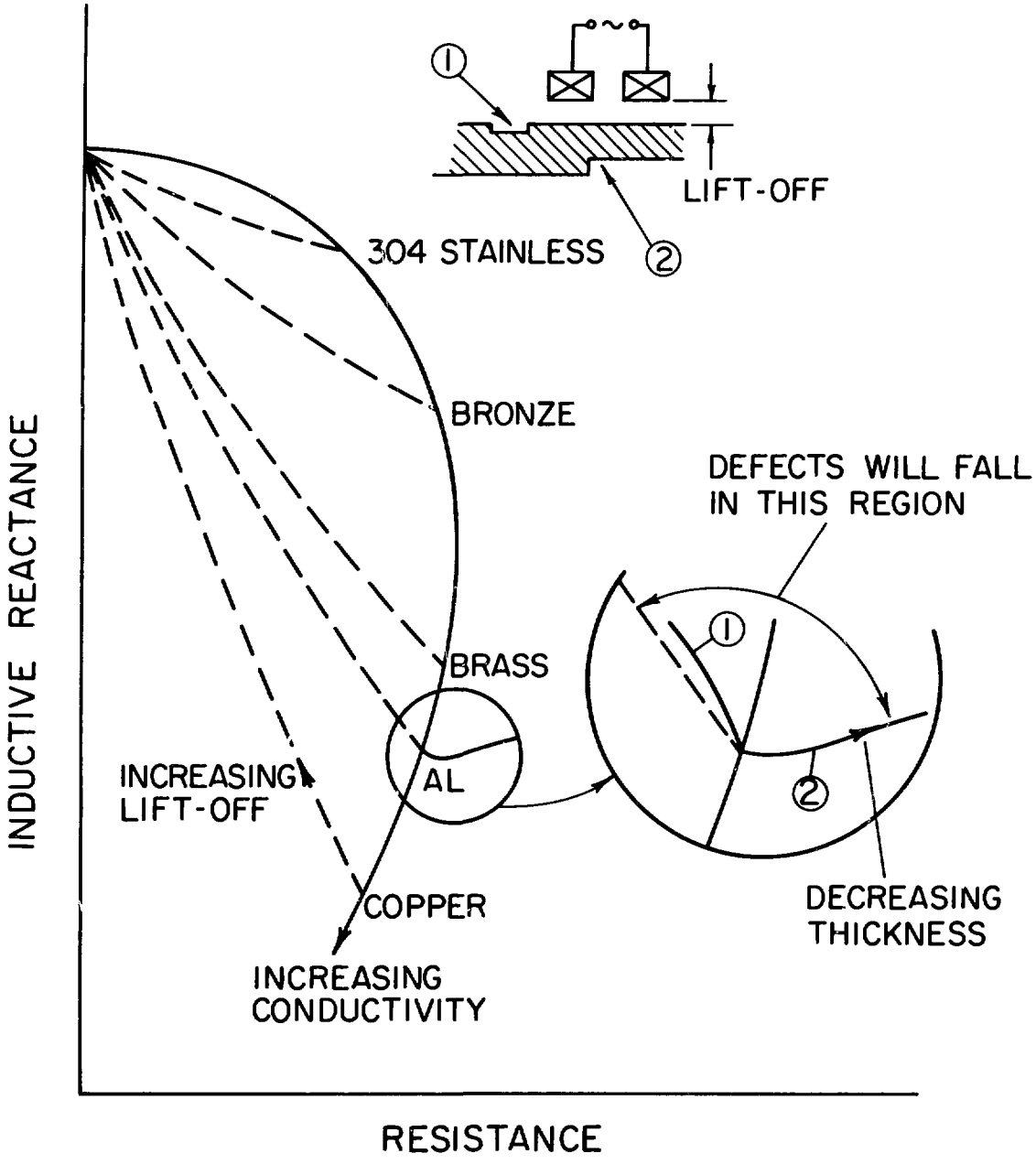

IMPEDANCE GRAPH DISPLAY

FIGURE 4 Impedance of a Surface Probe in Contact with Materials of Different Resistivity

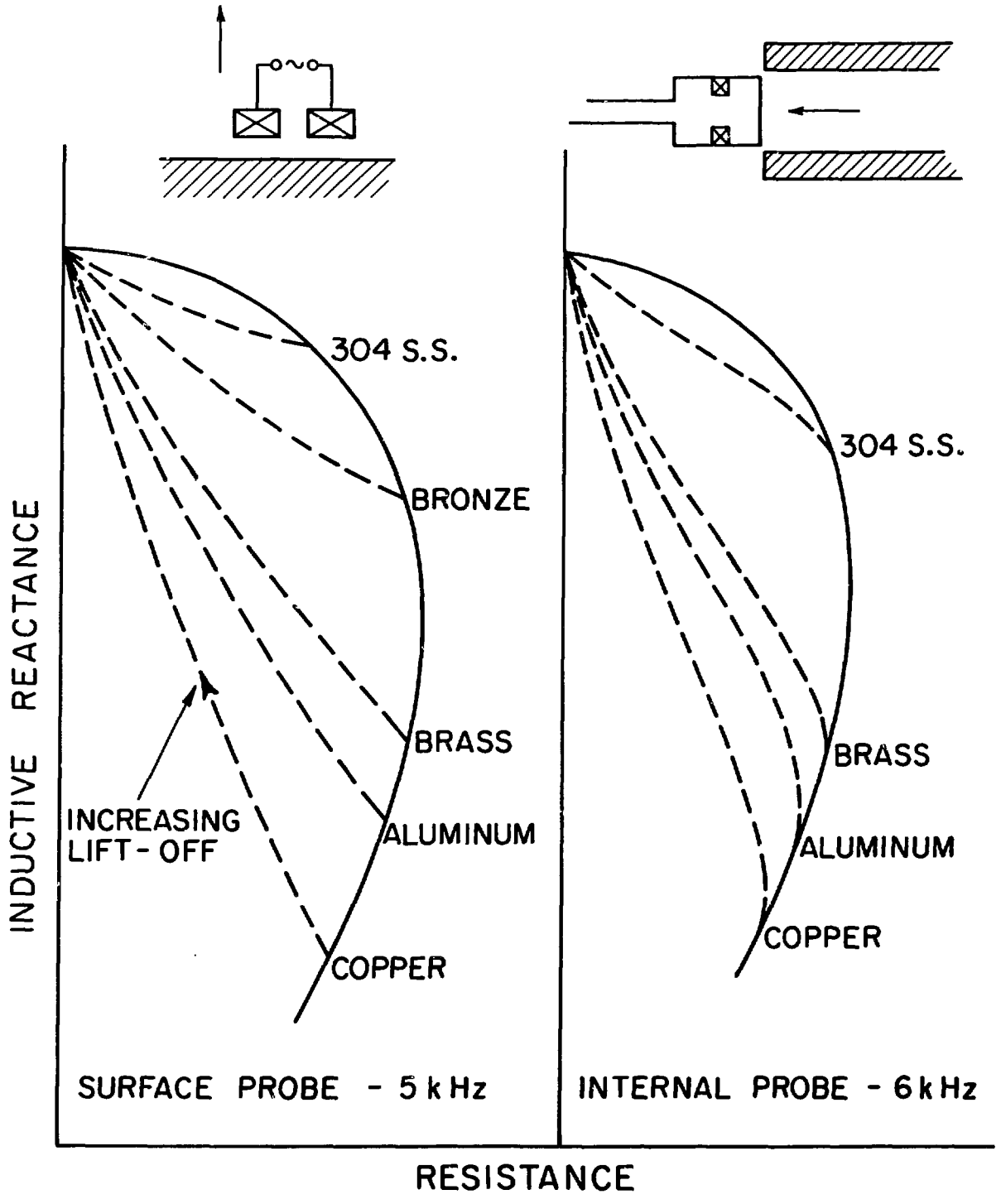

FIGURE 5 Comparison of Impedance Displays Obtained with Surface and Internal Probes (The arrows in the upper figures indicate direction of probe travel corresponding to the arrows on the impedance diagrams)

CALIBRATION DEFECTS

MATERIAL: Stainless Steel Tube
O.D. - 15.9 mm
Wall - 1.3 mm
Resistivity - 74 μΩ.cm

TEST PARAMETERS: Frequency - 128 kHz
Probe - Absolute, I.D.

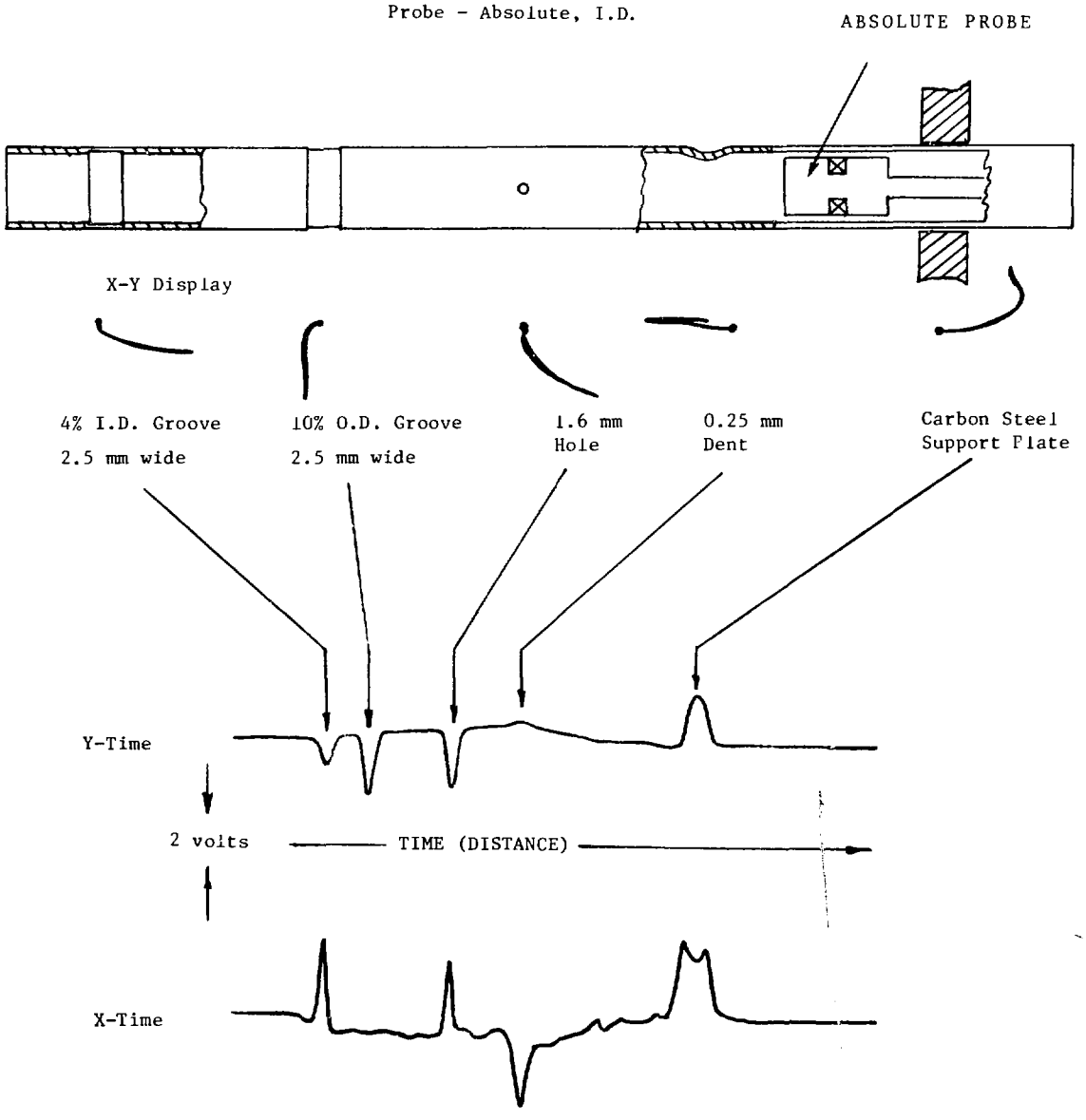

FIGURE 6 Eddy Current Signals from a Typical Calibration Tube with an Absolute Probe

MATERIAL: Copper Tube
O.D. - 15.9 mm
Wall - 1.0 mm
Resistivity - 1.8 μΩ.cm

TEST PARAMETERS: Frequency - 5.3 kHz
Probe - Absolute I.D.

(a)

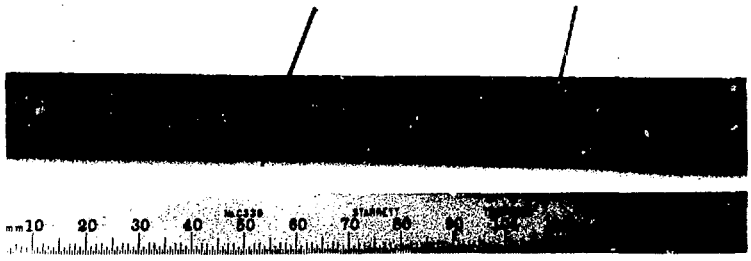

(b) CALIBRATION DEFECTS

0.25 mm Deep
Eccentric O.D. Groove

1.6 mm Hole

0.1 mm Deep
Eccentric I.D.
Groove

(c) CORROSION DEFECTS

Measured Depths

0.5 mm

0.5 mm

0.75 mm

FIGURE 7 External Corrosion in a Copper Tube

MATERIAL: Type 316 S.S. Tube
O.D. - 19.1 mm
Wall - 1.8 mm
Resistivity - 75 μΩ.cm

TEST PARAMETERS: Frequency - 68 kHz
Probe - Absolute, I.D.

(a)

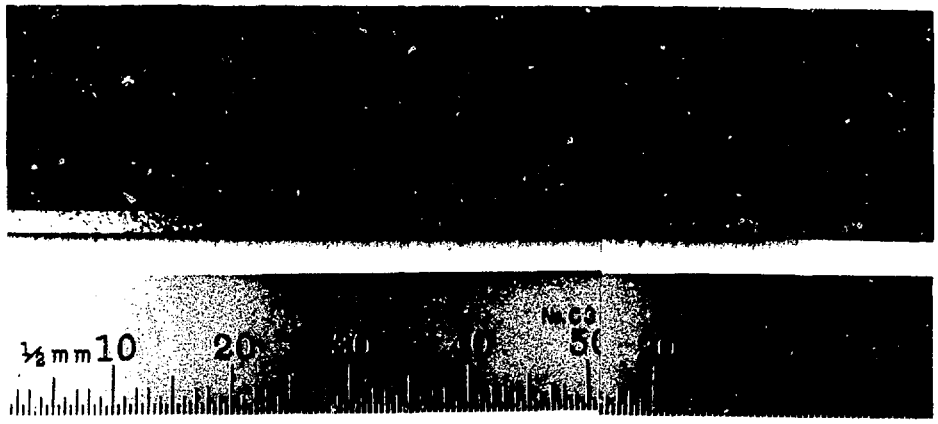

(b) CALIBRATION DEFECTS

0.5 mm O.D. Groove

1.6 mm Hole

0.1 mm I.D. Groove

(c) CORROSION DEFECTS

Measured 0.2 mm Depths

0.5 mm

0.4 mm

FIGURE 8 Internal Pitting Corrosion in Stainless Steel

MATERIAL: Brass Tube
O.D. - 15.9 mm
Wall - 1.0 mm
Resistivity - 8.25 μΩ.cm

TEST PARAMETERS: Frequency - 27.5 kHz
Probe - Absolute, I.D.

(a)

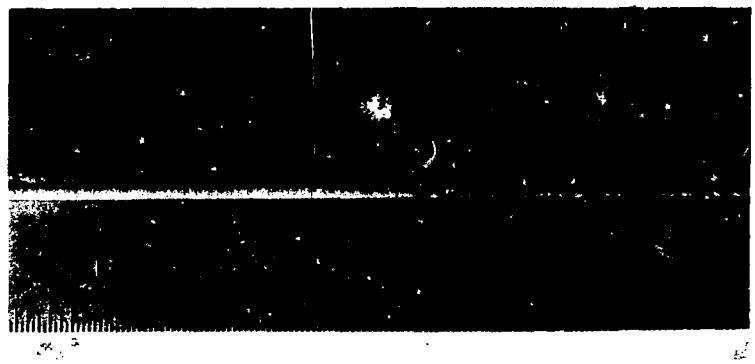

(b) CALIBRATION DEFECTS

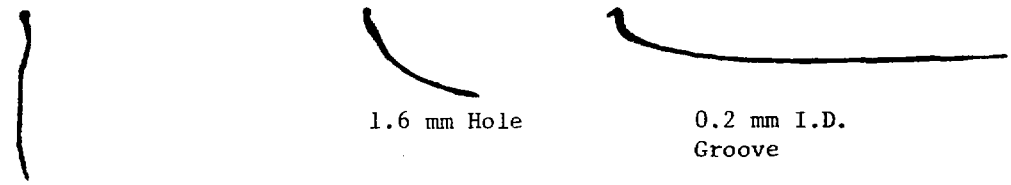

(c) CORROSION DEFECTS

FIGURE 9 General Internal Pitting in a Brass Tube

MATERIAL: Type 316 S.S. Tube
O.D. - 19.1 mm
Wall - 1.8 mm
Resistivity - 74 μΩ.cm

TEST PARAMETERS: Frequency - 68 kHz
Probe - Absolute, I.D.

(a)

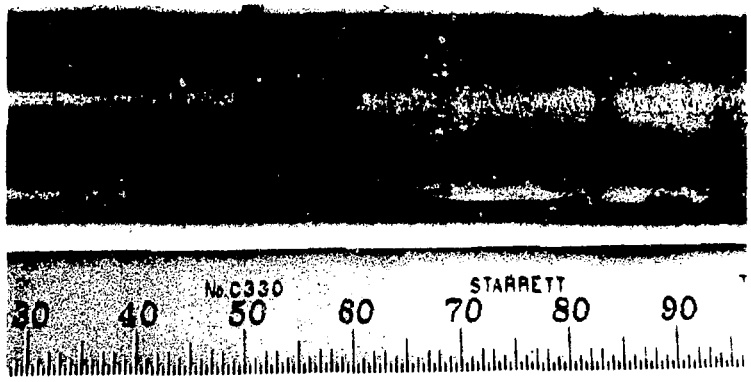

(b) CALIBRATION DEFECTS

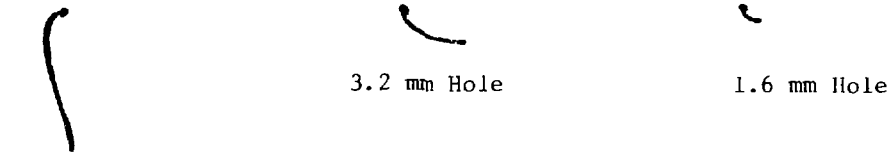

0.9 mm O.D. Groove

3.2 mm Hole

1.6 mm Hole

(c)

CRACK SIGNAL

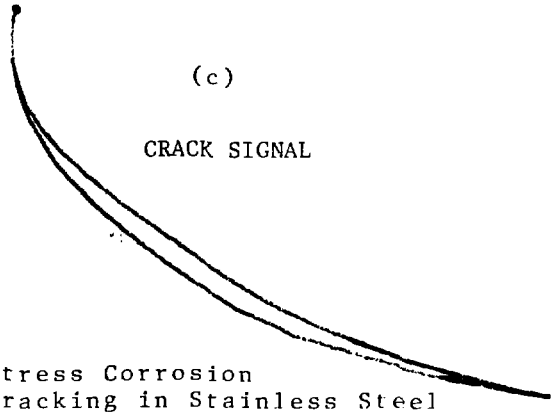

FIGURE 10 Stress Corrosion Cracking in Stainless Steel

MATERIAL: Brass Tube
O.D. - 22.1 mm
Wall - 1.1 mm
Resistivity - 9 μΩ.cm

TEST PARAMETERS: Frequency - 21 kHz
Probe - Absolute, I.D.

(a)

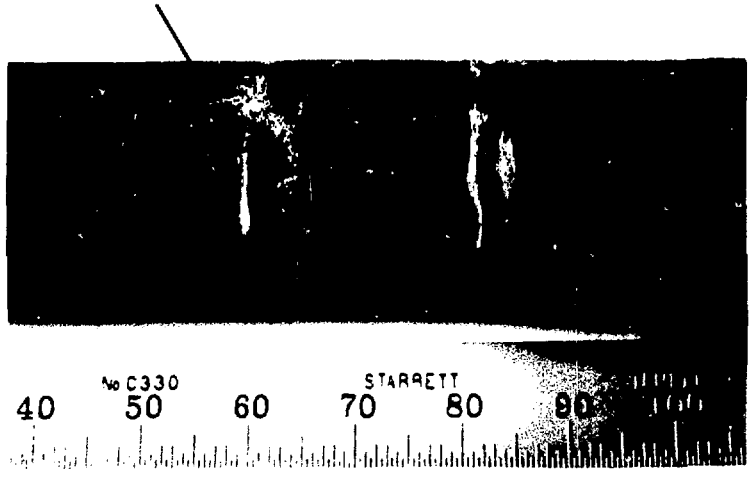

(b) CALIBRATION DEFECTS

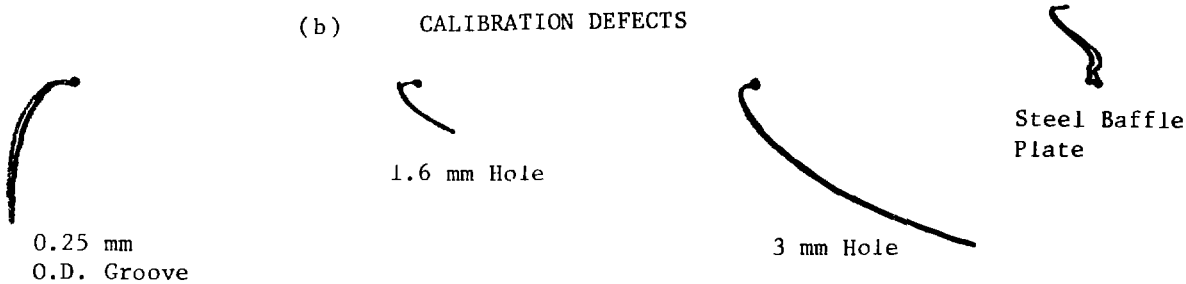

(c) DEFECT SIGNAL
(Baffle Plate & Defect)

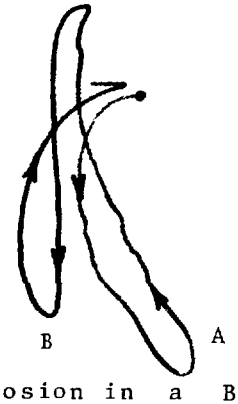

FIGURE 11 Erosion/corrosion in a Brass Heat Exchanger Tube

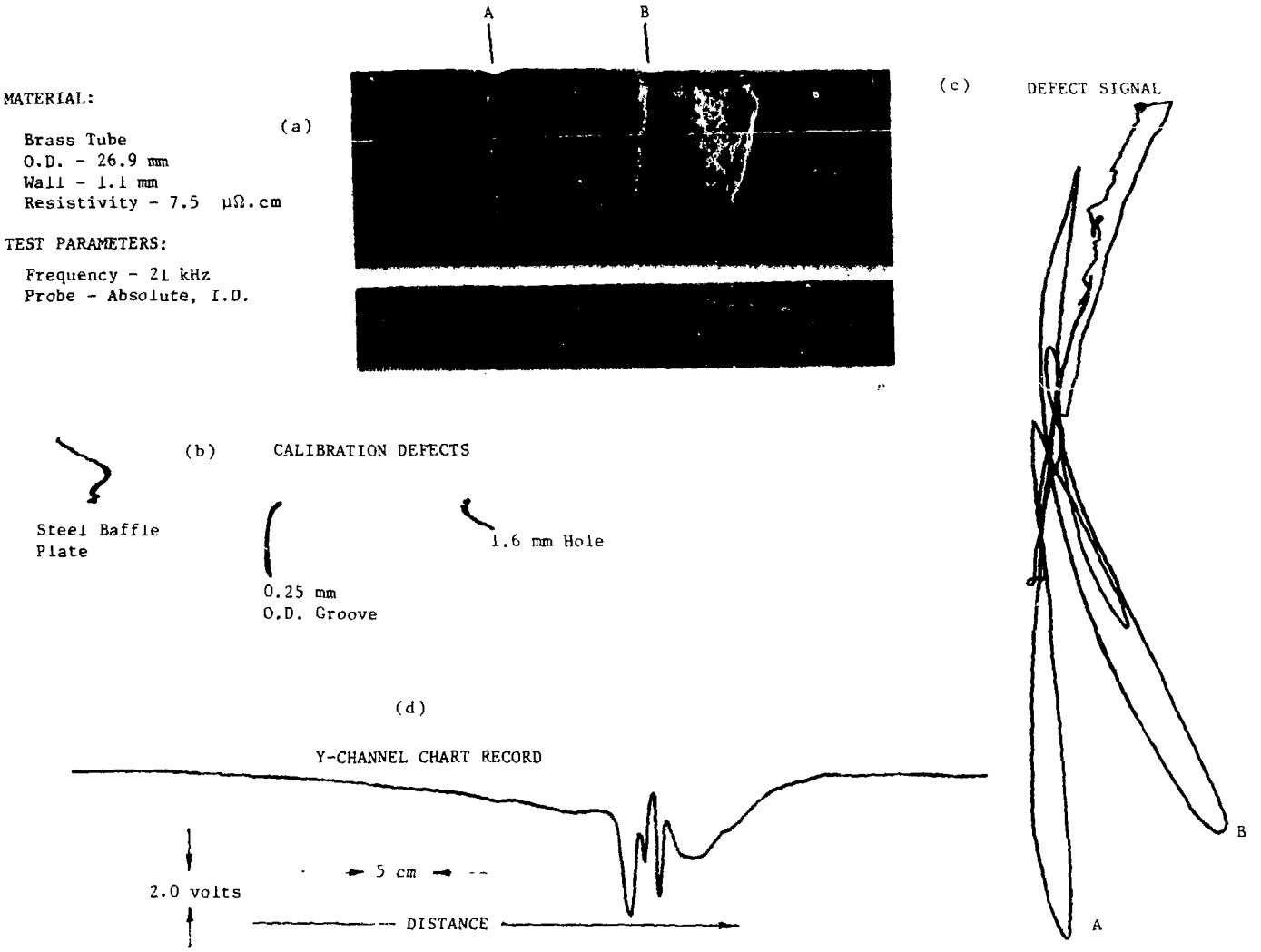

FIGURE 12 Erosion/corrosion in a Brass Tube Tested with an Absolute Probe

MATERIAL:

Brass Tube
O.D. - 26.9 mm
Wall - 1.1 mm
Resistivity - 7.5 μΩ,cm

TEST PARAMETERS

Frequency - 21 kHz
Probe - Differential, I.D.

CALIBRATION DEFECTS

(a)

0.25 mm
O.D. Groove

1.6 mm
Hole

(b) DEFECT SIGNAL

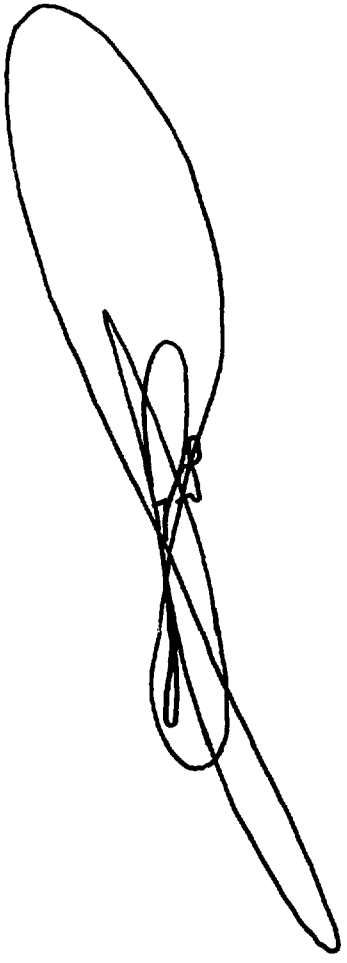

(c) Y-CHANNEL CHART RECORD

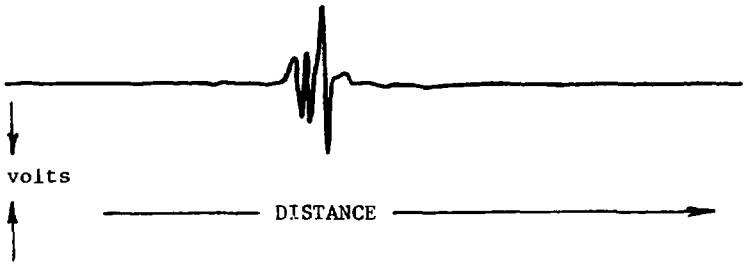

FIGURE 13 Same tube as Figure 12 Tested with a Differential Probe

MATERIAL: Type 316 S.S. Tube
O.D. - 15.9 mm
Wall - 1.3 mm
Resistivity - 74 μΩ.cm

TEST PARAMETERS: Frequency - 128 kHz
Probe - Absolute, I.D.

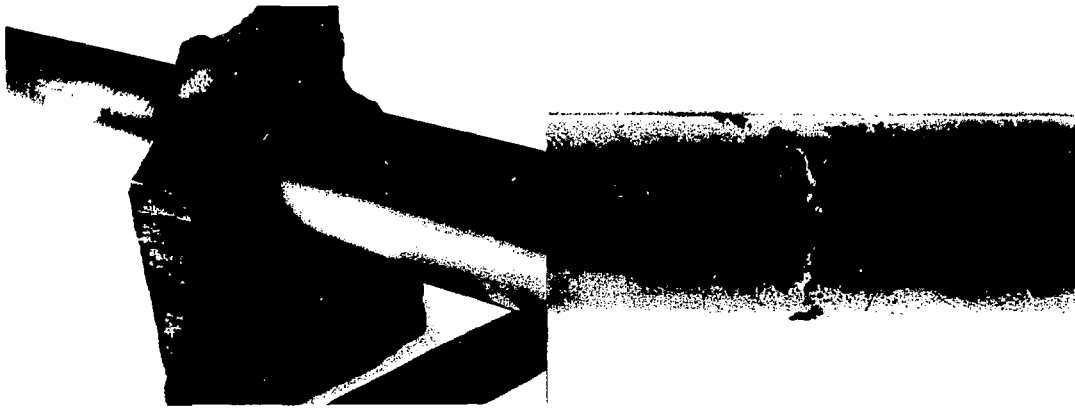

(a) (b)

(c) CALIBRATION DEFECTS

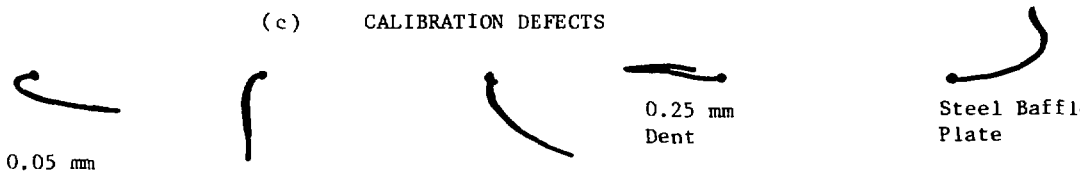

(d) DEFECT SIGNALS

FIGURE 14 Crevice corrosion with Denting under a Carbon Steel Support Plate

MATERIAL: Cu base alloy Tube
O.D. - 19 mm
Wall - 1.1 mm
Resistivity - 23 μΩ.cm

TEST PARAMETERS: Frequency - 54 kHz
Probe - Absolute and Differential, I.D.

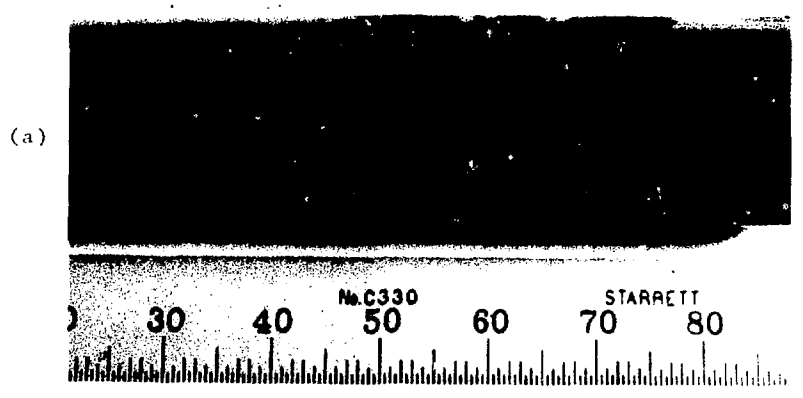

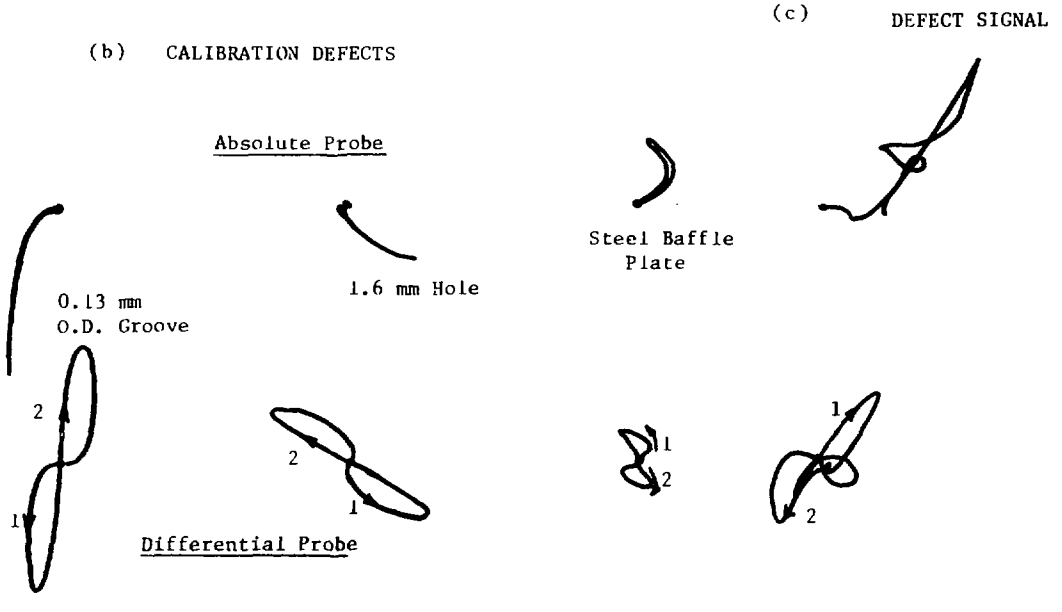

FIGURE 15 Eddy Current Signals from Copper Deposits on a Heat Exchanger Tube

MATERIAL: Inconel 600 Tube
O.D. - 13 mm
Wall - 1.1 mm
Resistivity - 98 μΩ.cm

TEST PARAMETERS: Frequency - Various
f_{90^o} = 240 kHz
Probe - Absolute, O.D.

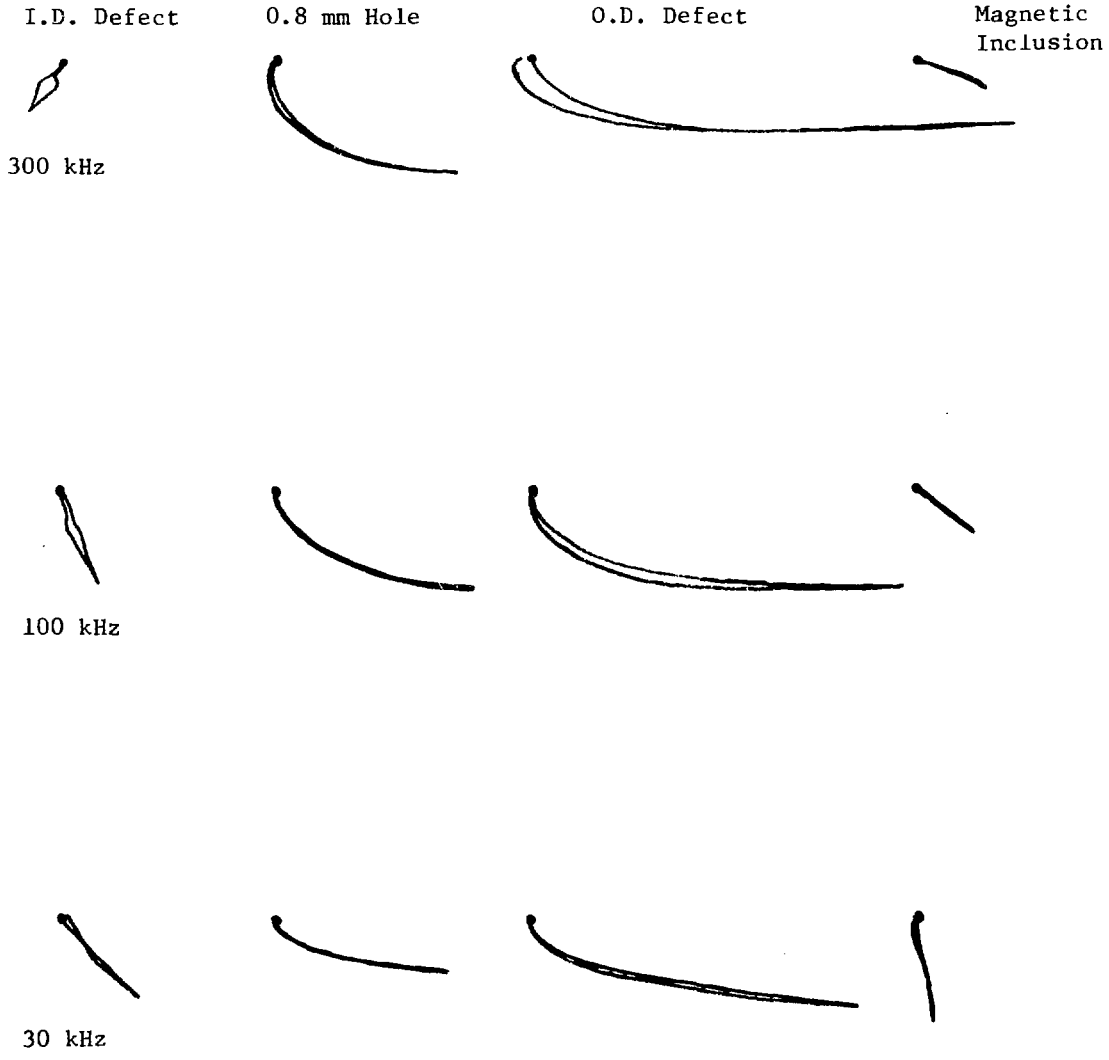

FIGURE 16 Eddy Current Signals from a Ferromagnetic Inclusion in a new heat Exchanger Tube

MATERIAL: Inconel 600 Tube
O.D. - 13.0 mm
WALL - 1.1 mm
RESISTIVITY - 98 μΩ.cm

TEST PARAMETERS: FREQUENCY - various
f_{90} = 250 kHz
PROBE - Absolute, I.D.

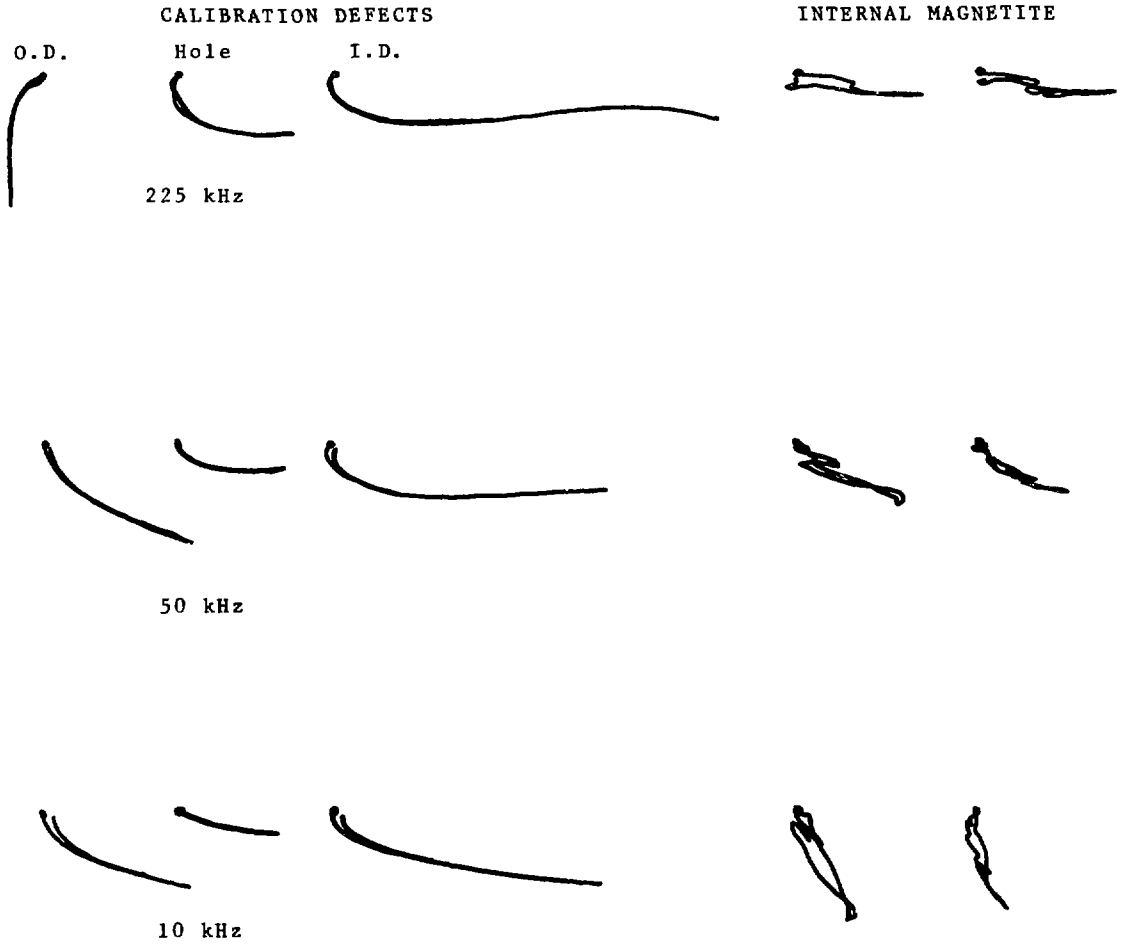

FIGURE 17 Eddy Current Indications from Magnetite Deposits Inside a Tube

ISSN 0067 - 0367

To identify individual documents in the series we have assigned an AECL- number to each.

Please refer to the AECL- number when requesting additional copies of this document

from

Scientific Document Distribution Office
Atomic Energy of Canada Limited
Chalk River, Ontario, Canada
K0J 1J0

Price $3.00 per copy

ISSN 0067 - 0367

Pour identifier les rapports individuels faisant partie de cette série nous avons assigné un numéro AECL- à chacun.

Veuillez faire mention du numéro AECL- si vous demandez d'autres exemplaires de ce rapport

au

Service de Distribution des Documents Officiels
L'Energie Atomique du Canada Limitée
Chalk River, Ontario, Canada
K0J 1J0

Prix $3.00 par exemplaire